Hindawi
Journal of Sensors
Volume 2021, Article ID 6634455, 9 pages
https://doi.org/10.1155/2021/6634455

Research Article

A Study of Highly Sensitive Wearable Strain Sensor Based on Graphical Sensitive Units

Jie Wang,[1] Yi Du,[1,2] Qiang Zhang,[1] Zhu Jing,[1] Kai Zhuo,[1] Jianlong Ji,[1] Zhongyun Yuan,[1] Wendong Zhang,[1] and Shengbo Sang[1]

[1]*Micro Nano System Research Center, Key Laboratory of Advanced Transducers and Intelligent Control System of Ministry of Education and Shanxi Province & College of Information and Computer, Taiyuan University of Technology, Taiyuan 030024, China*
[2]*Institute of Optoelectronic Thin Film Devices and Technology, Key Laboratory of Optoelectronic Thin Film Devices and Technology of Tianjin, College of Electronic Information and Optical Engineering, Nankai University, Tianjin 300350, China*

Correspondence should be addressed to Shengbo Sang; sunboa-sang@tyut.edu.cn

Received 23 November 2020; Revised 13 January 2021; Accepted 20 January 2021; Published 4 February 2021

Academic Editor: Xavier Vilanova

Copyright © 2021 Jie Wang et al. This is an open access article distributed under the Creative Commons Attribution License, which permits unrestricted use, distribution, and reproduction in any medium, provided the original work is properly cited.

The sensitivity improvement is the choke point of the soft strain sensor's development. This paper focuses on heightening the soft strain sensor's sensitivity through changing the sensitive unit's shape. The sensitive units in shape of square or sine wave with different periods were studied in this work. Silver nanowires (Ag NWs) in excellent electrical conductivity and flexible polydimethylsiloxane (PDMS) were used as sensitive nanomaterials and soft substrate. The soft strain sensor whose sensitive unit is double cycled square wave performs the highest sensitivity whose gauge factor (GF) reaches to 14763.8. Based on the high sensitivity, the sensor was applied on real-time detection of the human expression.

1. Introduction

Recently, the enthusiasm for flexible sensor research is intensifying, and the soft sensors have been applied on soft robot, E-skin health monitor, and so on [1–5]. However, some key problems such as low sensitivity, graphical appearance, and small range of application are overcoming to improving the soft sensors' properties [6–10]. Thus, more sensitive and graphical flexible strain sensors are research hotspots. Based on the soft strain sensors with better performances, the application range can be greatly widen [11–14].

Carbon-based nanomaterials, such as carbon nanotubes, graphenes, and graphene oxides with good mechanical properties have attracted great attention. As shown in Table 1, graphene in different patterns has been investigated as sensitive units of the flexible strain sensors, and the GFs are 29 and 35 based on PDMS and rubber substrates, respectively [15, 16]. The GF of the soft strain sensor composed by carbon nanotubes and PDMS is 0.97 [17]; thus, some researchers trying to improve the sensitivity via introducing different carbon nanomaterials. Branched carbon nanotubes and graphene nanoplatelets were mixed as sensitive unit to gain a higher GF at 144 [18]. Compared with carbon nanomaterials, acting as sensitive unit of soft strain sensor and mental nanomaterials such as Ag nanomaterials shows better performance in sensitivity improvement [15–21]. Moreover, the Ag nanomaterials' advances shown as mature synthesis method and excellent conductivity. The flexible strain sensors based on Ag NWs/elastic elastomer and Ag NWs/PU were demonstrated that the GFs are 70 and 81, respectively [19, 20]. Although the GF of the Ag NW-based soft strain sensors are higher than carbon nanomaterials, some researchers have been put their eyes on further improving the sensitivity via changing the morphology of the Ag nanomaterials. The GFs of the Ag nanocrystal and zigzag-shaped Ag nanoplate-based strain sensors reached to 312 and 2000, respectively [22].

In this work, the soft strain sensor's sensitivity was heightened through changing the sensitive unit's shape. The sensitive units in shape of square wave or sine wave with different periods and amplitudes were studied through investigating the piezoresistive performances of the sensors. High

Table 1: Research status of the strain sensors based on nanomaterials.

Nanomaterials	Substrate	GF	Reference
Fragmentized graphene foam	PDMS	29	15
Graphene	Rubber	35	16
Carbon nanotubes	PDMS	0.97	17
Carbon structures	TPU	144	18
Ag nanowires	Elastic elastomer	81	19
Ag nanowires	PU	70	20
Ag nanocrystal	PET	312	21
Zigzag-shaped Ag nanoplates	PDMS	2000	22

conductive Ag NWs and flexible PDMS were used as sensitive unit and soft substrate. The piezoresistive sensing model of sensors based on different shape sensitive units were established to explore the mechanism of sensitivity improvement. Finally, the soft strain sensor based on sensitive unit in the square wave structure with double cycles was applied on human expression detection.

2. Experimental

2.1. Preparation of Flexible Strain Sensors. The preparation process of the sensor is shown in Figure 1(a). First, prepare PDMS with rectangular grooves (purchased from Dow Corning, USA) by the template method. Ag NWs (purchased from Changsha Weixi New Materials Co., Ltd.) were dispersed in absolute ethanol (analytical grade, purchased from Tianjin Beichen Foundry Reagent Factory). The morphology of Ag NW was observed by FESEM (field emission scanning electron microscope, Japan Electronics JSM-7100F). After the PDMS is cured, the Ag NW solution dispersed in absolute ethanol is uniformly filled in the groove. After the absolute ethanol in the groove is volatilized, a rectangular silver layer is formed in the groove. Ag NWs are aggregated together and deposited on the substrate due to the cohesive force generated by the evaporation of absolute ethanol. Then, the copper electrode is fixed on the narrow end of the silver layer, and the Ag NWs and the copper electrode are connected with conductive silver paste. At the same time, due to the strong viscosity of the conductive silver paste, the two can be combined stably, reducing the impact of the contact resistance of the sensor during stretching. Finally, PDMS is used to encapsulate the Ag NWs, and PDMS is used as a protective layer to protect the piezoresistive material layer during the stretching process and ensure the stability of the sensor. After the PDMS is cured, a flexible film with a sandwich structure is prepared (sensor 1). The shapes of the sensors' sensitive units are shown in Figure 1(b), and sensor 1 to sensor 7 were fabricated to investigate the performances of the sensors.

2.2. Characterization. The current-voltage curves were measured by the Keithley 2400 Source Meter at room temperature. Stretching experiments were carried out on the stretching platform (Zolix TSM25-1A and Zolix TSMV60-1 s, Zolix Corporation, Beijing, China), and the resistance of the sensors was measured by Keithley 2400 Source Meterat. The resistance changes of the most sensitive sensor during surprised, confused, smiling, angry expressions were characterized by the Keithley 2400 Source Meter.

3. Results and Discussion

The electrical characteristics of the sensor are characterized, and the ohmic characteristics of the sensor are detected by current-voltage curves of the sensors.

The cross-sectional size of the sensor is shown in Figure 2(a), and the thickness of the conductive material is about 20-30 μm. As shown in Figure 2(b), the Ag NWs were uniformly dispersed, and the nanowires had a diameter of 50 nm and a length of 20 μm. Figure 2(c) shows the resistance changes of seven devices. The current-voltage curves of the seven different sensors are smooth straight lines, all with good ohmic characteristics. The resistance of sensor 1 is 0.9 Ω, which indicates that the soft strain sensor with rectangular sensitive cells has excellent conductivity. The resistances of 3 and 4 are 8.55 Ω and 8.3 Ω, respectively, which is slightly lower than the 9.42 Ω of sensor 2. Comparing the shape of the sensitive unit of these three sensors, the resistance is related to the period on the same horizontal length. The resistances of sensors 5, 6, and 7 are 3238.8 Ω, 806.45 Ω, and 4454.45 Ω, respectively. Different from the sensor with the square wave-shaped sensitive unit, the sensor with the sinusoidal-shaped sensitive unit has a closer relationship between resistance and length. At the same time, the direction of the conductive path is a key factor in the conductivity of the sensor, and a conclusion can be drawn by comparing sensors 2, 3, and 4 with sensors 5, 6, and 7. This means that lower resistance depends on the composition direction of the conductive path and the applied electric field. In order to confirm the conductive network formed by Ag NWs, the morphology of Ag NWs was observed by SEM.

The relationship between resistance and strain range is shown in Figure 3(b). The schematic diagram of sensor 1, whose sensitive unit is a rectangular square wave, is shown in Figure 4(a). The resistance increasing owing to sensitive unit's deformation and tunneling effect. The resistance expression is expressed as equation 1, where ρ is the resistivity of the material (the international unit system is Ω, m), L is the length of the resistance (the international unit system is meters, m), and S is the conductor wire cross-sectional area (the international unit system is square meters, m^2). The conductive path of the sensitive unit becomes longer and narrower, so the resistance increases according to $R = \rho(L/S)$. Besides, cracks' distances of the nanomaterials increase during stretching. The electrons can tunnel through the polymer matrix and form a quantum conductive junction when the crack distance is smaller than the distance between two neighboring nanomaterials and 30 times higher than the distance of a single nanomaterial. Those are the reasons that the resistance of sensor 1 increases from 0 to 46.8 Ω during stretching in the X direction, which is shown in Figure 4(b), when the sensitive unit is a rectangular strip. When the sensor is stretched in the X direction, the resistance of the sensor exhibits an increasing tendency based

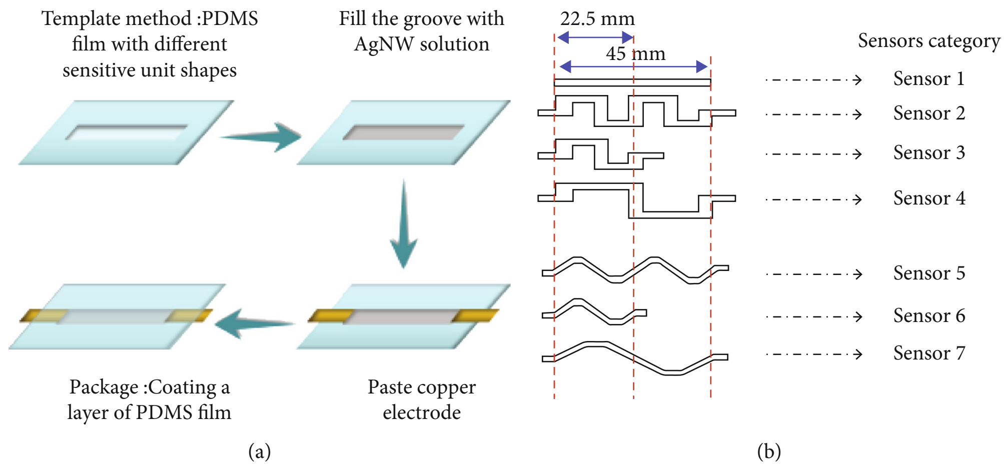

Figure 1: (a) Sensor preparation process. (b) Different shapes of sensitive units.

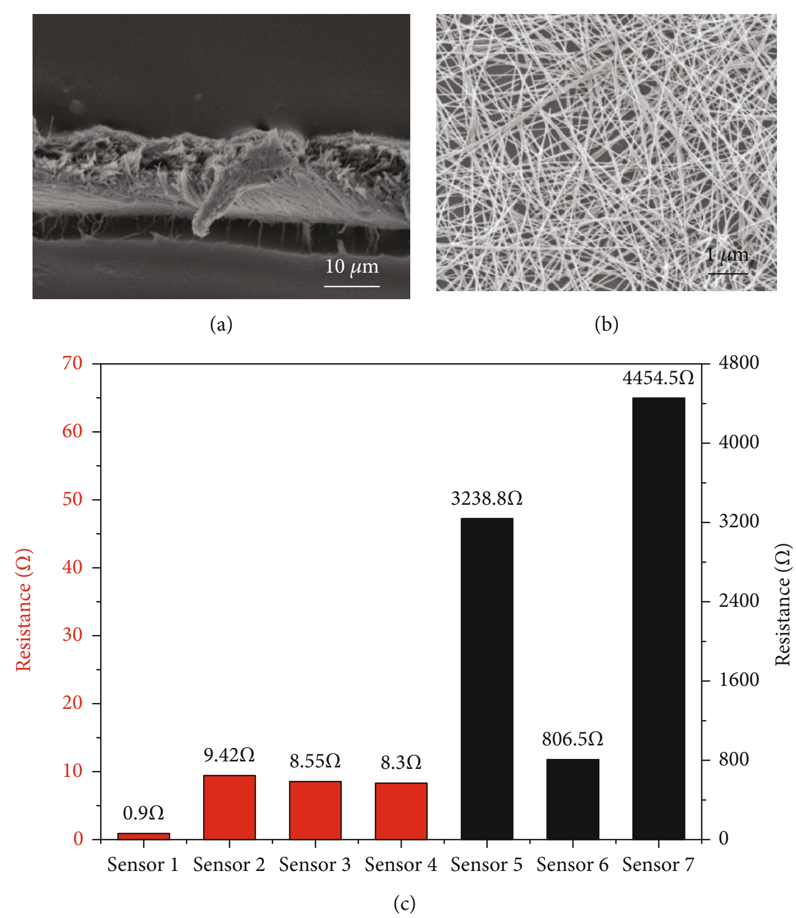

Figure 2: Ohmic characteristic curve of different sensors. (a) SEM image of sensor cross-section. (b) SEM of the sensitive units Ag NWs. (c) The relationship between sensitive units' shapes and as-prepared sensors' resistances.

on the increases of L and decrease of S, and the tunneling effect occurs along the stretching direction. If the sensor is stretched in the Y direction, the resistance tends to decrease due to decrease of L and increase of S, so this decrease trends of resistance change were abandoned to measure in this work. The gauge factor (GF) is defined as equation 2, where ΔR is the relative resistance change under the deformation, R_0 is the initial resistance of the sensor, ΔL is the relative elongation of the axial specimen, and L_0 is the initial length of the sensor. The GF of sensor 1 was calculated as 544.2 according to $GF = \Delta R/R_0/\Delta L/L_0$.The schematic diagram of sensors 2-4 whose sensitive units are rectangular square wave

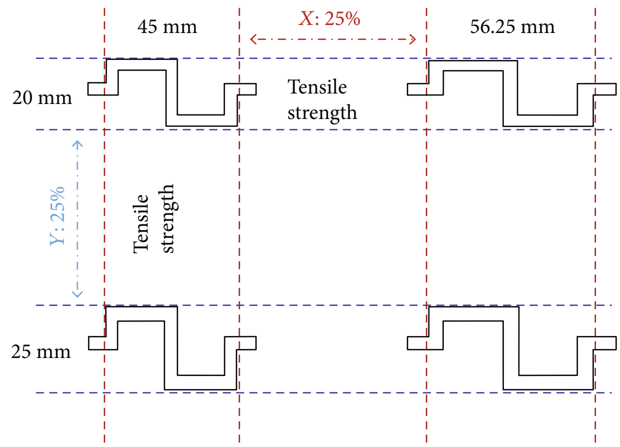

(a)

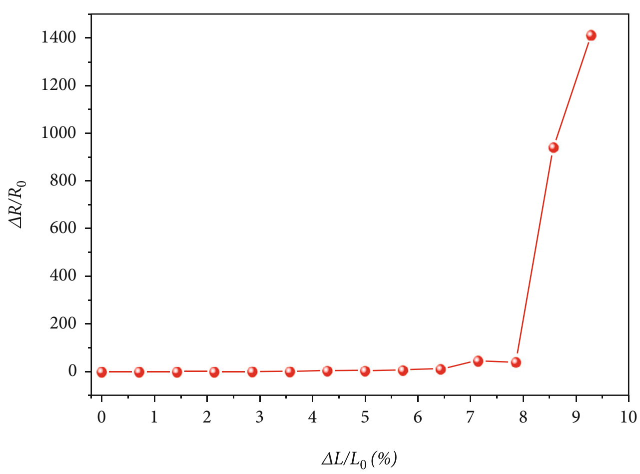

(b)

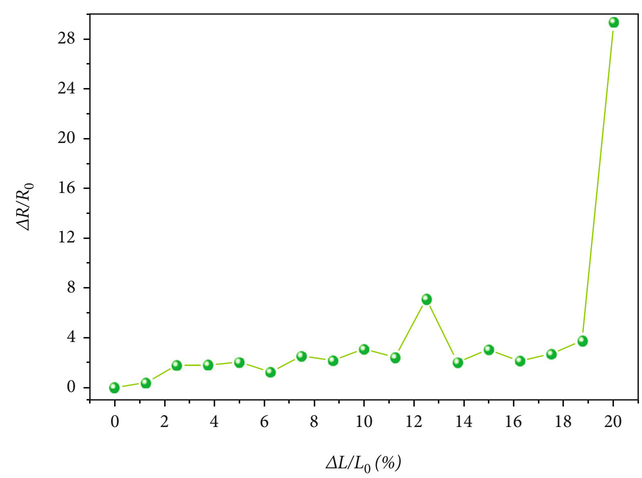

(c)

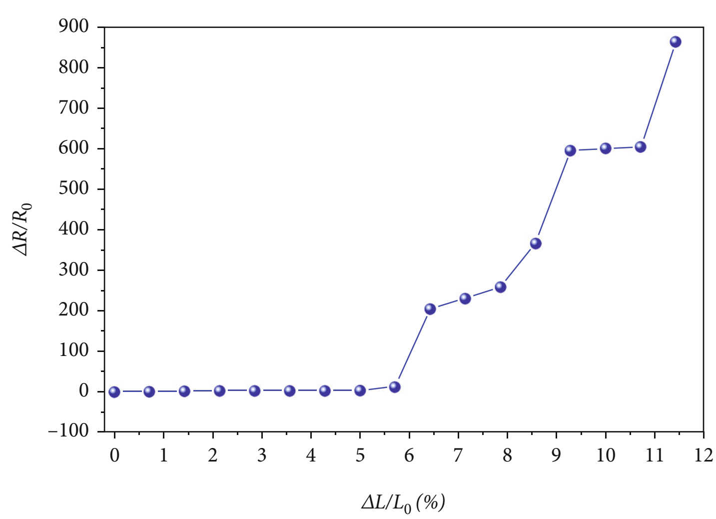

(d)

Figure 3: (a) Sensor stretching schematic diagram of square waved sensitive units. (b) Tensile characteristic curve of sensor 2. (c) Tensile characteristic curve of sensor 3. (d) Tensile characteristic curve of sensor 4.

is shown in Figure 3(a) during stretching. When the sensor is stretched in the X direction, the conductive path of the sensitive unit becomes longer and narrower, so the resistance increases. When the sensor is stretched in the Y direction, the conductive path of the sensitive unit becomes shorter and wider, which leads to the reduce of the resistance. Therefore, the resistance changes of the sensors stretching along the X direction are studied, and results are shown in

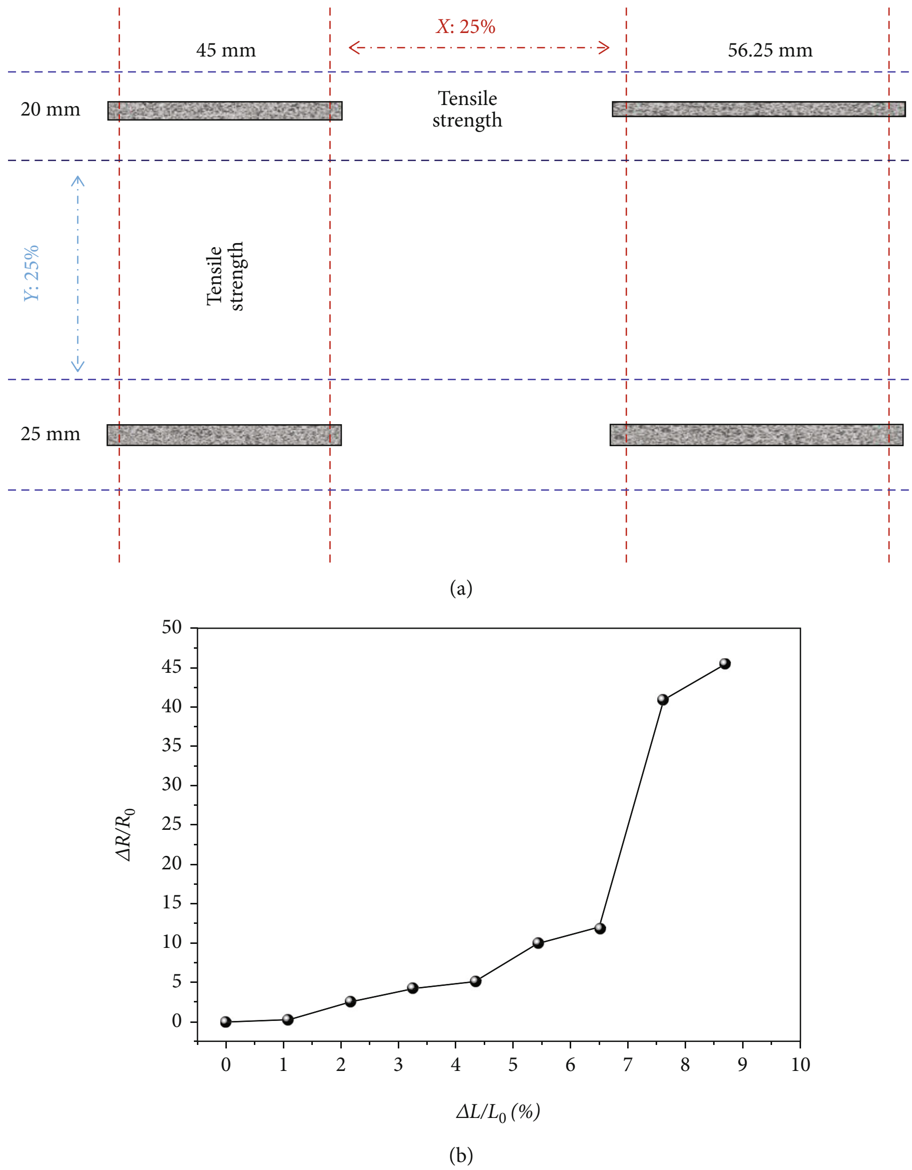

FIGURE 4: (a) The schematic diagram of the rectangular sensitive unit. (b) Corresponding sensor 1 tensile characteristic curve.

Figures 3(b)–3(d). The stretching range and the GF of the sensor 2, whose sensitive unit is two rectangular wave periods, are 9.5% and 14763.8, respectively. The GF of sensors 2 and 3 with one rectangular wave period sensitive unit in different lengths exhibits 140 and 7391.3 during 20% and 11.5% stretching. The sensor 2's sensitive unit is longer than the other two sensors; thus, the sensitive unit's length changes more during stretching. That is the reason that the sensitivity of sensor 2 is the highest. Besides, the nanomaterials in sensor 2 are more than sensors 3 and 4, which leads to larger tunneling resistance during deformation. The sensing range of the sensor 3 is wider when comparing with sensors 1, 2, and 4. This phenomenon is owning to the shortest initial length in the Y axis of the sensor 3, and the relative length change means larger $\Delta L/L_0$. The wider sensing range of the sensor 4 than sensor 2 demonstrates the corners' negative effect for sensing range during stretching.

Figure 5(a) shows the schematic diagram of the sensor with the sinusoidal sensitive unit. The conductive path of the sensitive unit becomes longer and narrower during stretching in the X direction, so the resistance increases. Figures 5(b)–5(d) represent the resistance changes of the sensors 5-7 during stretching. The GF of sensor 5 with two sine wave periods sensitive unit is 13636.4 during 5.7% stretching. However, the resistance does not increase gradually with stretching. In the contrast, the resistances of the sensor 6 and 7, which the sensitive unit is one sine wave periods, increase gradually during stretching. The GF of sensor 6 is 450 during 10% stretching, which is higher than that of sensor 6 in 307.7. The sensitivity and the strain range of the sensors with sinusoidal sensitive unit are both weaker than other sensors. Moreover, the resistance does not change gradually with deformation. The direction of the force is not parallel to the direction of the sensor sensitive unit, so the way of

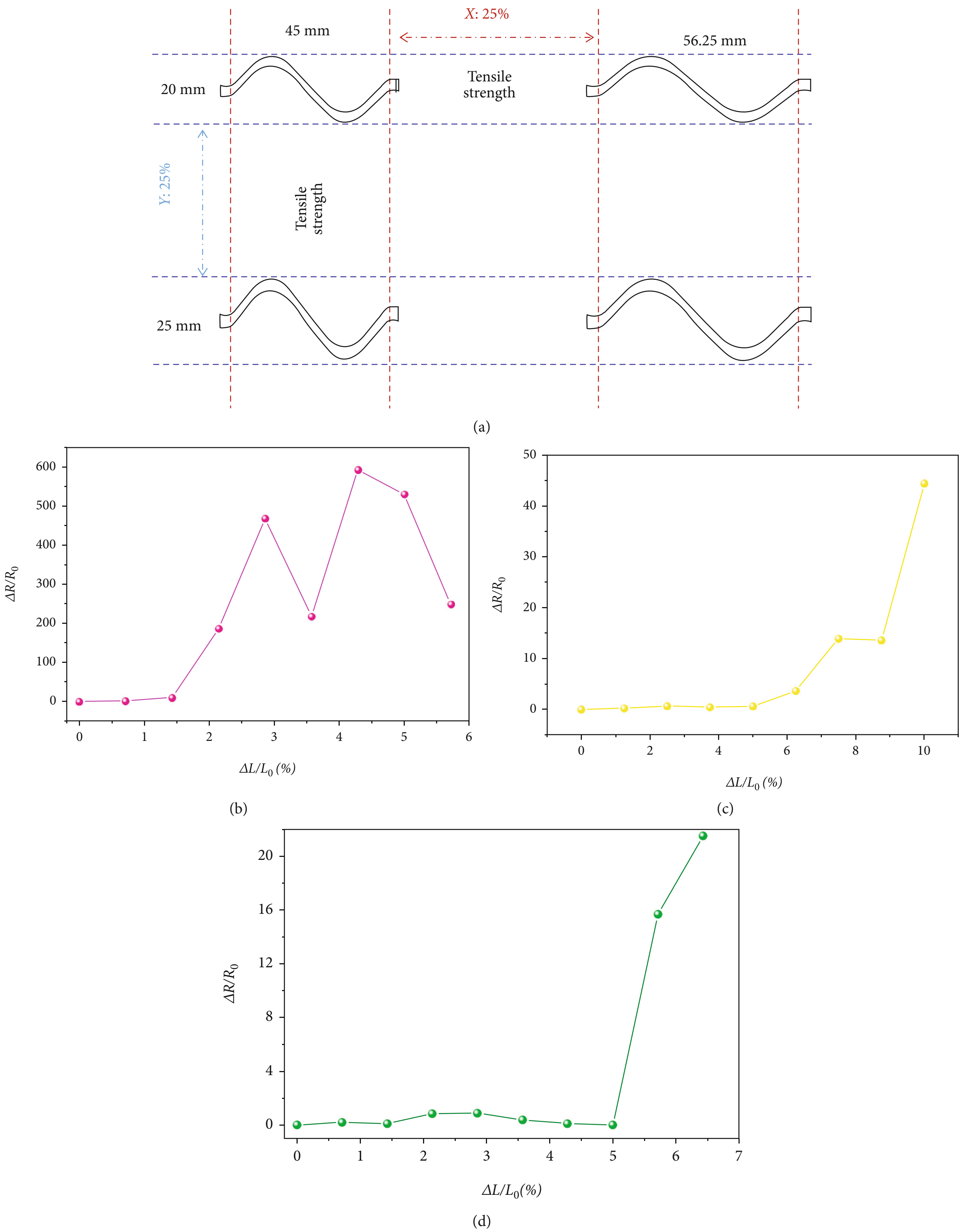

Figure 5: (a) Stretching schematic diagram of a sensor with a sinusoidal circular wave. (b) Tensile characteristic curve of sensor 5. (c) Tensile characteristic curve of sensor 6. (d) Tensile characteristic curve of sensor 7.

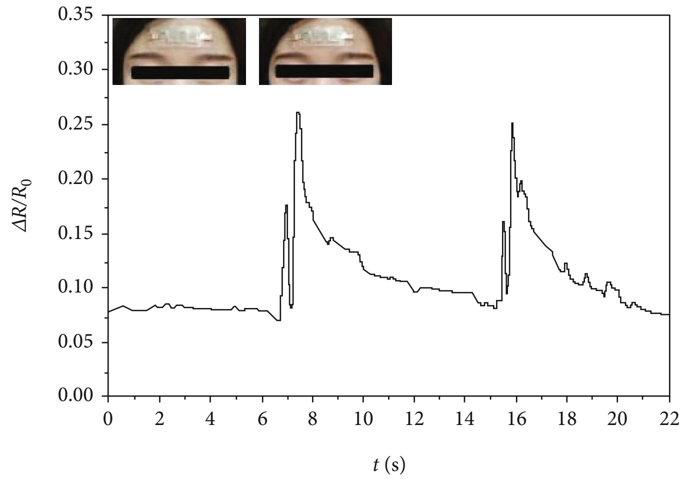

(a)

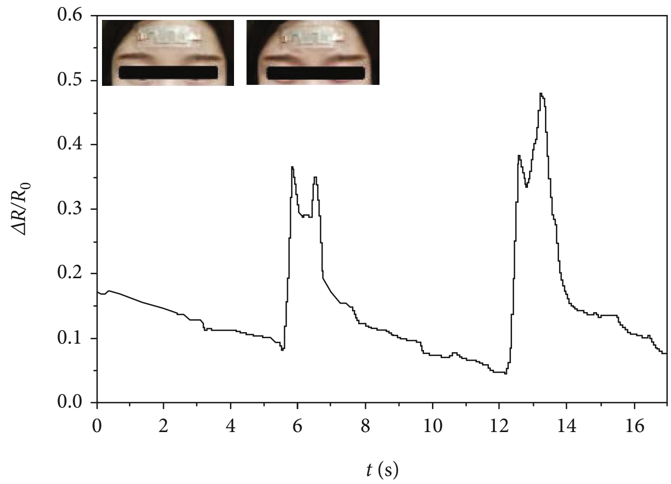

(b)

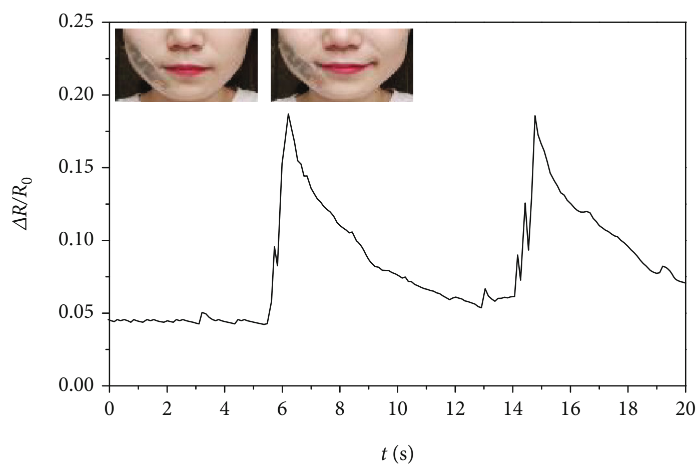

(c)

Figure 6: Continued.

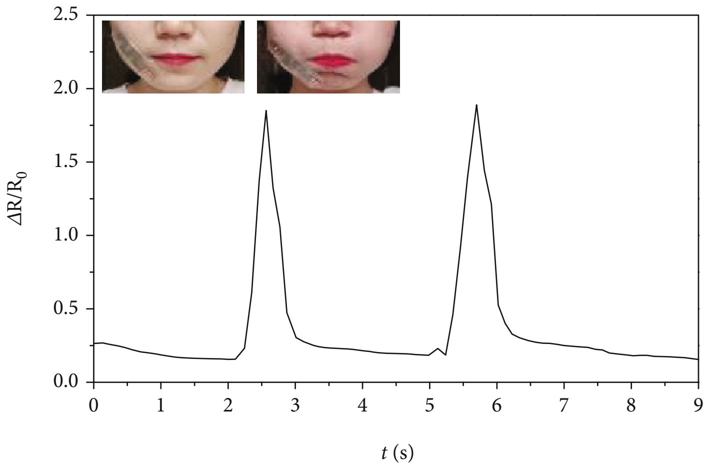

(d)

Figure 6: Expression recognition on the forehead. (a) Surprised expression. (b) Confused expression. (c) Expression recognition of the mouth smile expression. (d) Angry expression.

the nanomaterials separating from each other and reforming the conductive path is irregular in the stretching process. The strain range of the sensor 6 seems in range of sensors 1 and 2, while the initial length in the Y axis of is the shortest. Therefore, the relative longer strain range is not owing to the sensor's performance. In other words, the performance of sensors with sine wave period sensitive units is poor.

In summary, the graphical study of the sensor sensitive unit helps to improve the sensitivity of the sensor, and the sensitivity of the sensor with square waved sensitive unit is 27 times larger than sensor with simple rectangular sensitive unit. Compared with other sensors with different sensitive unit shapes, the detection range of the sensor with double rectangular waved sensitive unit is $0 \sim 10\%$, and the highest GF of the sensor is 14763.8. Thus, this sensor is selected as the flexible device for the expression recognition application. When the sensor was attached to the forehead of the human body along the X direction, the experimenter made a surprised expression and a confused expression. The resistance changes of the sensor with volunteer's expression changes are shown in Figures 6(a) and 6(b). The distance between the eyes becomes larger when the human makes a surprised expression as shown in Figure 6(a). The surprising expression causing the muscles of the forehead stretching the sensor, and the resistance increases during this process. When the volunteer makes a confused expression as shown in Figure 6(b), most part of the sensor was stretched while a short length of the sensor shrieked, so the resistance of the sensor increased first. During keeping the confused expression, the muscle tremor is the source of the slightly contraction of the sensor. Therefore, the resistance has a small process of sudden decrease during the process of resistance increasing. When the sensor was attached besides the mouth, the resistance changes with the volunteer's happy expression and angry expression were shown in Figures 6(c) and 6(d). When the human face makes a smiling expression, the resistance increases with the sensor stretching with the movement of the face. The resistance returns to the initial value at a slow speed as the face slowly returns to the normal state. The sensor rapidly stretching as the face bulging rapidly when the human face makes an angry expression; thus, the resistance increases in this process. After the expression ends, the face quickly returns to the normal state. This process is faster than the smile on the facial expression. The muscle movement of the smiling is in the largest range, so the peaks of the resistance changing during the angry expression are the highest.

4. Conclusion

This study focuses on heightening the soft strain sensor's sensitivity through increasing the sensitive units' length in the same volume. The sensitive units in shape of square wave or sine wave with different periods and amplitudes were studied in this work. The graphical study of the sensor sensitive unit helps to improve the sensitivity of the sensor, and the sensitivity of the sensor with square waved sensitive unit is 27 times larger than the sensor with simple rectangular sensitive unit. The soft strain sensor based on sensitive unit in square wave structure with double cycle performs the highest sensitivity, whose GF reached to 14763.8. The flexible sensor was applied on real-time detection of the human expression based on its high sensitivity.

5. Statement

The experiment was carried out with the consent of the experimenter, and the experiment did not have substantial contact with the human body.

Data Availability

All data, models, and code generated or used during the study appear in the submitted article.

Conflicts of Interest

The author(s) declare(s) that they have no conflicts of interest.

Authors' Contributions

Jie Wang and Yi Du contributed equally to this work.

Acknowledgments

This study was financially supported by the Basic Research Program of Shanxi Province (No. 201901D111097).

References

[1] Z. Jing, Q. Zhang, Y. Cheng et al., "Highly sensitive, reliable and flexible piezoresistive pressure sensors based on graphene-PDMS@ sponge," *Journal of Micromechanics and Microengineering*, vol. 30, no. 8, Article ID 085012, 2020.

[2] Q. Zhang, W. Jia, C. Ji et al., "Flexible wide-range capacitive pressure sensor using micropore PE tape as template," *Smart Materials and Structures*, vol. 28, no. 11, Article ID 115040, 2019.

[3] P. Won, J. J. Park, T. Lee et al., "Stretchable and transparent kirigami conductor of nanowire percolation network for electronic skin applications," *Nano Letters*, vol. 19, no. 9, pp. 6087–6096, 2019.

[4] P. Li, D. Zhang, J. Wu, Y. Cao, and Z. Wu, "Flexible integrated black phosphorus sensor arrays for high performance ion sensing," *Sensors and Actuators B: Chemical*, vol. 273, pp. 358–364, 2018.

[5] L. B. Gao, K. Cao, X. K. Hu et al., "Nano electromechanical approach for flexible piezoresistive sensor," *Applied Materials Today*, vol. 18, article 100475, 2020.

[6] R. K. Mishra, A. Barfidokht, A. Karajic, J. R. Sempionatto, J. Wang, and J. Wang, "Wearable potentiometric tattoo biosensor for on-body detection of G-type nerve agents simulants," *Sensors and Actuators B: Chemical*, vol. 273, pp. 966–972, 2018.

[7] S. Hong, J. Yeo, J. Lee et al., "Selective laser direct patterning of silver nanowire percolation network transparent conductor for capacitive touch panel," *Journal of Nanoscience and Nanotechnology*, vol. 15, no. 3, pp. 2317–2323, 2015.

[8] Y. Gu, T. Zhang, H. Chen et al., "Mini review on flexible and wearable electronics for monitoring human health information," *Nanoscale Research Letters*, vol. 14, no. 1, p. 263, 2019.

[9] B. Liang, Z. Lin, W. Chen et al., "Ultra-stretchable and highly sensitive strain sensor based on gradient structure carbon nanotubes," *Nanoscale*, vol. 10, no. 28, pp. 13599–13606, 2018.

[10] Z. Wang, H. Zhou, J. Lai et al., "Extremely stretchable and electrically conductive hydrogels with dually synergistic networks for wearable strain sensors," *Journal of Materials Chemistry C*, vol. 6, no. 34, pp. 9200–9207, 2018.

[11] S. J. Kim, S. Mondal, B. K. Min, and C. G. Choi, "Highly sensitive and flexible strain–pressure sensors with cracked paddy-shaped MoS_2/graphene foam/ecoflex hybrid nanostructures," *ACS Applied Materials & Interfaces*, vol. 10, no. 42, pp. 36377–36384, 2018.

[12] T. Yan, Z. Wang, and Z. J. Pan, "A highly sensitive strain sensor based on a carbonized polyacrylonitrile nanofiber woven fabric," *Journal of Materials Science*, vol. 53, no. 16, pp. 11917–11931, 2018.

[13] C. J. Lee, K. H. Park, C. J. Han et al., "Crack-induced Ag nanowire networks for transparent, stretchable, and highly sensitive strain sensors," *Scientific Reports*, vol. 7, no. 1, article 7959, 2017.

[14] Y. L. Wang, Y. Y. Jia, Y. J. Zhou et al., "Ultra-stretchable, sensitive and durable strain sensors based on polydopamine encapsulated carbon nanotubes/elastic bands," *Journal of Materials Chemistry C*, vol. 6, no. 30, pp. 8160–8170, 2018.

[15] Y. R. Jeong, H. Park, S. W. Jin, S. Y. Hong, S. S. Lee, and J. S. Ha, "Highly stretchable and sensitive strain sensors using fragmentized graphene foam," *Advanced Functional Materials*, vol. 25, no. 27, pp. 4228–4236, 2015.

[16] C. S. Boland, U. Khan, C. Backes et al., "Sensitive, high-strain, high-rate bodily motion sensors based on graphene-rubber composites," *ACS Nano*, vol. 8, no. 9, pp. 8819–8830, 2014.

[17] L. Cai, L. Song, P. Luan et al., "Super-stretchable, transparent carbon nanotube-based capacitive strain sensors for human motion detection," *Scientific Reports*, vol. 3, no. 1, p. 3048, 2013.

[18] K. Ke, V. Solouki Bonab, D. Yuan, and I. Manas-Zloczower, "Piezoresistive thermoplastic polyurethane nanocomposites with carbon nanostructures," *Carbon*, vol. 139, pp. 52–58, 2018.

[19] K. H. Kim, N. S. Jang, S. H. Ha, J. H. Cho, and J. M. Kim, "Highly sensitive and stretchable resistive strain sensors based on microstructured metal nanowire/elastomer composite films," *Small*, vol. 14, no. 14, article 1704232, 2018.

[20] C. S. Boland, U. Khan, H. Benameur, and J. N. Coleman, "Surface coatings of silver nanowires lead to effective, high conductivity, high-strain, ultrathin sensors," *Nanoscale*, vol. 9, no. 46, pp. 18507–18515, 2017.

[21] S. W. Lee, H. Joh, M. Seong, W. S. Lee, J. H. Choi, and S. J. Oh, "Engineering surface ligands of nanocrystals to design high performance strain sensor arrays through solution processes," *Journal of Materials Chemistry C*, vol. 5, no. 9, pp. 2442–2450, 2017.

[22] J. Kim, S. W. Lee, M. H. Kim, and O. O. Park, "Zigzag-shaped silver nanoplates: synthesis via ostwald ripening and their application in highly sensitive strain Sensors," *ACS Applied Materials & Interfaces*, vol. 10, no. 45, pp. 39134–39143, 2018.